

**MINISTRY OF EDUCATION  
AND TRAINING**

**VIETNAM ACADEMY OF SCIENCE  
AND TECHNOLOGY**

**GRADUATE UNIVERSITY OF SCIENCE AND TECHNOLOGY**

---



**Tang Xuan Duong**

**RESEARCH ON FABRICATION AND CONTROL OF  
ELECTROMAGNETIC WAVE ABSORPTION  
PROPERTIES IN THE GHz FREQUENCY RANGE  
BASED ON MAGNETIC MATERIALS (FeCo and MFe<sub>2</sub>O<sub>4</sub>)  
AND METAMATERIALS**

**SUMMARY OF DISSERTATION ON MATERIALS SCIENCE**

**Major: Electronic material**

**Code: 9 44 01 23**

**Ha Noi - 2026**

The dissertation is completed at: Graduate University of Science and Technology, Vietnam Academy Science and Technology

Supervisors:

1. Supervisor 1: Prof. Dr. Vu Dinh Lam, Viet Nam National Space Center, Vietnam Academy Science and Technology
2. Supervisor 2: Dr. Bui Son Tung, Graduate University of Science and Technology, Vietnam Academy Science and Technology

Referee 1: Assoc. Prof. Dr. Le Dac Tuyen, School of Electrical and Electronic Engineering, Hanoi University of Industry.

Referee 2: Assoc. Prof. Dr. Pham Hong Minh, Institute of Physics, Vietnam Academy of Science and Technology.

The dissertation is examined by Examination Board of Graduate University of Science and Technology, Vietnam Academy of Science and Technology at 09.00 May 15<sup>th</sup>, 2026

The dissertation can be found at:

1. Graduate University of Science and Technology Library
2. National Library of Vietnam

## INTRODUCTION

### 1. The urgency of the dissertation

In the context of rapid digital transformation driven by next-generation wireless communication systems (5G and the emerging trend toward 6G) and the widespread deployment of the Internet of Things (IoT), the density of electromagnetic fields/radiation in daily living and working environments has been increasing rapidly, due to the growing number of transmitting sources and electro-electronic devices operating in the microwave range [1 - 5]. The impact of electromagnetic exposure on biological systems continues to attract attention and is being investigated through both modeling and experimental studies. In the defense and security domain, the requirement to control electromagnetic emissions is closely associated with stealth technology, aiming to reduce the radar cross section of platforms against modern reconnaissance systems that primarily operate in the GHz band. Therefore, developing solutions for electromagnetic shielding/interaction mitigation has become an essential need in many applications [6, 7].

To meet these requirements, electromagnetic wave absorption materials (EMWAMs) have been intensively studied with the goal of converting electromagnetic energy into heat through intrinsic loss mechanisms. Depending on the dominant mechanism, EMWAMs are generally classified into three groups: dielectric absorbers; resistive/conductive (lossy) absorbers; and magnetic absorbers. Each group has its own advantages: dielectric materials are often favorable for impedance matching; carbon-based/conductive materials provide strong dielectric (conductive) loss and low density; while magnetic materials (ferrites, magnetic metals, magnetic alloys, etc.) can simultaneously improve impedance matching and dissipate energy through magnetic permeability, and are therefore particularly important in the GHz regime [9, 10]. However, the “strong, broadband, lightweight, and thin” target [11] is difficult to achieve simultaneously: purely dielectric materials lack magnetic loss channels, so their GHz performance depends strongly on optimizing permittivity together with thickness; carbon-based/conductive materials can

suffer from degraded impedance matching, leading to increased surface reflection and secondary pollution/interference [12, 13]; meanwhile, Fe-/metal-based magnetic materials may offer strong absorption but are often heavy, prone to oxidation, and difficult to impedance-match with air, resulting in narrow absorption bandwidths or challenges in achieving high absorption at small thicknesses.

The current demand is not only for high absorption, but also for optimized bandwidth, reduced sensitivity to polarization and incident angle, and, in particular, the capability for active tuning of the absorption frequency. On this basis, metamaterials (MM) open up a structure-driven design approach, notably metamaterial absorbers (MA), first proposed by Landy and co-workers in 2008 [19]. Although MAs have been demonstrated from the microwave to the optical regime, practical deployment still faces several fundamental challenges: reducing fabrication complexity while maintaining high absorption; improving stability with respect to polarization and incident angle; broadening the operating band (multi-resonant or broadband designs); and developing mechanisms to control the absorption frequency under external stimuli. In the GHz range, approaches such as integrating multiple resonant elements or using multilayer MAs can broaden the absorption spectrum [24], but this often comes at the cost of a larger unit-cell size or a thicker structure, thereby undermining the “thin–lightweight” advantage. Solutions based on external components (resistors, capacitors, etc.) can help tune impedance and resonance [25], yet they significantly increase fabrication complexity. One promising research direction to overcome these limitations is to incorporate intrinsically lossy materials into MA to enhance and broaden the absorption region. In particular, integrating magnetic materials into MA structures to form magnetic–metamaterial composite absorbers (Composite based on Magnetic material-Metamaterial Absorbers, CM-MA) has attracted considerable attention from researchers. Globally, broadband-absorbing CM-MA composites currently mainly employ magnetic materials in the form of coating layers, using various material systems such as carbonyl iron, ferrites, FeCo-C, and CoNi/epoxy, among others [26-30]. However, studies on optimizing the thickness of CM-MA structures remain

limited, and the approach of using magnetic materials as resonant elements/structures has not yet been widely investigated. In addition, research on tuning the absorption spectrum has mainly focused on shifting the absorption frequency, typically using  $\text{MgFe}_2\text{O}_4$  and YIG [27, 31, 32]. Meanwhile, other magnetic material systems for absorption control particularly amplitude modulate at a fixed frequency and multi-peak spectrum tuning-have not been thoroughly studied.

In Vietnam, research on magnetic materials for electromagnetic wave absorption and metallic resonant MA structures in the GHz range has been receiving increasing attention [33-36]. Various material systems, including Ni-Zn ferrites, hexaferrites, and magnetic-dielectric materials, have been investigated [37-39], along with several representative dissertations on electromagnetic wave absorbing materials and metamaterial absorbers [40-45]. Nevertheless, the research direction of integrating magnetic materials with metamaterials to achieve broadband absorption or to control absorption characteristics using an external magnetic field remains novel, non-overlapping with previous studies, and has strong potential for developing more efficient and flexible electromagnetic wave absorber systems.

For these reasons, the project entitled: Research on the fabrication and control of electromagnetic wave absorption properties in the GHz frequency range based on composites of magnetic materials ( $\text{FeCo}$  and  $\text{MFe}_2\text{O}_4$ ) and metamaterials” was chosen. The dissertation presents the achieved research results on the design and fabrication of several CM-MA using magnetic materials based  $\text{FeCo}$  for broadband electromagnetic wave absorption, and CM-MAs using magnetic materials based  $\text{MFe}_2\text{O}_4$  capable of independently modulating either the absorption intensity or the absorption frequency of the CM-MA by an external magnetic field; as well as evaluating the contributions and roles of the magnetic material and the metamaterial that constitute the composite material.

## **2. The objectives of the dissertation**

- Design and fabricate CM-MA composite materials capable of broadband absorption EMW in the GHz frequency range.

- Design and fabricate CM-MA composite materials whose EMW absorption characteristics can be actively tuned by an external magnetic field.

### **3. Content of the Research**

The dissertation integrates multiple research approaches, including theoretical calculations, numerical simulations, fabrication, and experimental characterization. After synthesis, the magnetic materials are characterized in terms of their electromagnetic parameters and subsequently implemented in CST Studio Suite for simulation. Metamaterial absorber (MA) specimens are fabricated using photolithography, and the magnetic materials are incorporated into the MA architecture via paraffin- and epoxy-based binders. The scope of the study primarily focuses on CM - MA composite materials for electromagnetic wave absorption.

### **4. Scientific and Practical Implications**

The dissertation is scientifically significant in establishing models of broadband metamaterial absorbers incorporating magnetic materials that enable control of the absorption amplitude and resonant frequency under an external magnetic field.

#### **Novel Contributions**

The dissertation has proposed and successfully fabricated CM-MA structures that broaden and enhance the absorption capability of magnetic materials by integrating them into MA structures. The absorption amplitude and resonance frequency of the magnetic-material-based metamaterial absorber can be tuned/modulated by an external magnetic field. The results demonstrate the application potential of CM-MA in electromagnetic shielding, energy harvesting, sensing, and related areas, serving both military–defense and civilian purposes.

#### **Thesis Structure**

The dissertation comprises 150 pages, including an Introduction, four content chapters, and the Conclusions.

## **CHAPTER 1. OVERVIEW OF COMPOSITE (MAGNETIC–METAMATERIAL) ABSORBERS OF ELECTROMAGNETIC WAVES**

### **1.1. Mechanisms of electromagnetic wave absorption in materials**

### **1.1.1. Magnetic loss mechanisms**

Magnetic losses comprise the main groups of mechanisms: ferromagnetic resonance, domain-wall resonance, eddy-current loss, hysteresis loss, and exchange resonance. Magnetic losses can be classified into two principal origins: intrinsic loss associated with the nature of the material and extrinsic loss related to shape, size, and the surrounding environment [52, 53].

### **1.1.2. Dielectric loss mechanisms**

Electromagnetic wave - absorbing materials are typically characterized by the combined contributions of conduction loss and polarization-relaxation loss. Microwave absorption characteristics depend not only on increasing  $\epsilon''$  but also strongly on polarization mechanisms across multiple scales (atomic-defect-microstructural), which can produce strong loss while still maintaining appropriate impedance matching [58, 59].

## **1.2. Magnetic material systems for electromagnetic wave absorption**

### **1.2.1. Soft magnetic materials for electromagnetic wave absorption**

Soft magnetic materials are characterized by a low coercive field ( $H_c$ ), medium-to-high saturation magnetization ( $M_s$ ), low hysteresis loss, and easy magnetization reversal under weak external magnetic fields. Owing to their high electrical resistivity and low eddy-current loss, soft ferrites are suitable for GHz-frequency applications, where pure metallic magnetic materials (Fe, Co, Ni) typically suffer from excessively large eddy-current losses. Among spinel ferrites, the Ni-Zn system ( $\text{Ni}_{1-x}\text{Zn}_x\text{Fe}_2\text{O}_4$ ) is one of the most extensively studied material families for microwave absorption due to its relatively high  $M_s$  and  $\mu'$ , resonance frequencies in the GHz range, high resistivity, and flexible tunability by varying the Ni/Zn ratio and additives/dopants [97-99].

Also within the soft magnetic absorbers operating in the GHz regime, FeCo alloys with their high saturation magnetization and large Snoek's limit help maintain good magnetic response in the microwave range. However, single-phase FeCo often exhibits disadvantages: (i) poor impedance matching due to the lack of dielectric loss mechanisms, and strong reflection

caused by high electrical conductivity; it is prone to oxidation; and its high density undermines the “thin - lightweight - broadband - strong absorption” criteria. Therefore, an effective approach is to hybridize FeCo with a carbon phase (amorphous carbon/graphitized carbon/graphite/graphene, reduced graphene oxide), forming a magnetic-dielectric system in which both  $\mu_r$  and  $\varepsilon_r$  can be tuned simultaneously, thereby optimizing absorption in the C–X–Ku bands (approximately 4 - 18 GHz) [100-106].

### **1.2.2. Hard magnetic materials for electromagnetic wave absorption**

Hard magnetic materials exhibit a large coercive field (high  $H_c$ ) and a wide hysteresis loop, making them suitable for permanent-magnet applications. In the context of electromagnetic wave absorption, an advantage of hard magnetic materials is that their natural magnetic resonance frequency can be extended to very high frequency ranges (up to tens to hundreds of GHz) due to their large anisotropy field [107]. M-type hexaferrite systems such as  $\text{BaFe}_{12}\text{O}_{19}$ ,  $\text{SrFe}_{12}\text{O}_{19}$ , La - Sr - M, etc., are typical representatives of oxide-based hard magnetic materials; they possess relatively high  $M_s$ , large  $H_c$ , and high chemical and thermal stability, making them suitable for harsh environments (temperature, radiation, corrosion) [97].

### **1.2.3. Hard-Soft magnetic materials**

Hard-soft magnetic materials are multiphase systems consisting of a hard magnetic phase (with large magnetocrystalline anisotropy and high coercivity  $H_c$ ) combined with a soft magnetic phase (with high saturation magnetization  $M_s$  but low  $H_c$ ), in which the phases are organized on the nanoscale to form exchange interactions at the phase boundaries [108]. Systems such as  $\text{BaFe}_{12}\text{O}_{19}/\text{Ni}_{0.5}\text{Zn}_{0.5}\text{Fe}_2\text{O}_4$ ,  $\text{BaFe}_{12}\text{O}_{19}/\text{Ni}_{0.8}\text{Zn}_{0.2}\text{Fe}_2\text{O}_4$ ,  $\text{SrFe}_{12}\text{O}_{19}/\text{CoFe}_2\text{O}_4$ ,  $\text{CoFe}_2\text{O}_4/\text{Fe}_3\text{O}_4$ ...etc., have been widely investigated, showing that exchange coupling between the two phases can broaden the resonance spectrum, thereby enabling wider absorption bandwidths and lower values of  $RL_{\min}$  [98, 109].

## **1.3. Metamaterial electromagnetic wave absorbers**

### **1.3.1. Impedance matching theory**

From a physical perspective, the absorption performance of MA originates from the interplay between strong electromagnetic resonances and impedance optimization in artificial structures. By designing periodically arranged metallic elements, the input impedance of the material can be tuned to approach the impedance of free space (air), leading to an almost complete cancellation of reflected waves. Maximum absorption is typically achieved by selecting the geometry and constituent materials such that the overall reactive component (imaginary part) of  $Z_{in}$  is driven close to zero and the real part approaches  $Z_0$ . Once the energy enters the structure, sufficiently large losses ensure that it is dissipated through dielectric, magnetic, and ohmic losses [119].

### **1.3.2. Destructive interference theory**

Interference theory emphasizes that the total reflection at the structure's entrance surface is not a single reflection event, but rather the superposition of multiple reflected components generated by multiple reflections within the cavity between the resonant-structure surface and the metal reflective layer underneath. Destructive interference only ensures a small external reflection; however, to achieve truly high absorption, the energy that has entered the material layer must be dissipated through loss mechanisms [118].

### **1.3.3. Resonance mechanisms in metamaterial structures**

Electric resonance occurs when the electric-field component  $E$  of the incident wave strongly excites the resonant elements of the MA structure. In this case, surface charges accumulate strongly in the gaps, creating an equivalent capacitance  $C$ ; simultaneously, induced currents flowing along the conductive paths generate an equivalent inductance  $L$ , leading to an LC-type resonance. This mechanism produces a Lorentz/Drude-Lorentz response for  $\epsilon_{eff}(\omega)$ . Electric resonance contributes to Joule loss (conversion into heat) and also helps satisfy the impedance-matching condition, thereby enabling electromagnetic wave absorption in the structure [121, 122].

Magnetic resonance arises when the magnetic-field component  $H$  excites the resonant element within the structure. Magnetic resonance is often formed by antiparallel surface currents between the top resonant layer

and the bottom reflective (ground) plane, generating a magnetic moment and a magnetic resonant response that contributes to the formation of absorption peaks [124].

Unlike MA based metal, MA based dielectric exploit displacement currents in high-refractive-index dielectric resonators (Si, TiO<sub>2</sub>, dielectric ceramics, ferroelectric/ceramic materials, etc.). When the resonator dimensions satisfy the condition of being comparable to the wavelength inside the material, Mie modes appear, in which the two lowest-order modes are typically the electric dipole (ED) and magnetic dipole (MD). The MD mode is produced by circulating displacement currents, whereas the ED mode is associated with the displacement-charge distribution aligned with the excitation direction. In certain frequency bands, dielectric MAs can simultaneously yield negative permeability and negative permittivity, resulting in absorption peaks [125].

By employing diverse structures, some studies have observed multiband absorption phenomena based on higher-order resonances [126].

#### **1.3.4. Metamaterial electromagnetic wave absorber structures**

MA have been widely discussed since the seminal proposal by Landy and co-workers (2008) [19]. Building on that foundation, by varying the geometric dimensions of the resonant unit cell and the shape/symmetry of the top metallic layer, one can actively control the positions and the number of absorption bands appearing in the spectrum. Alongside multiband designs, research has also strongly shifted toward broadband MAs, as broadband operation is a key requirement in many practical applications. Depending on absorption characteristics, MAs can be classified into three main groups: single-peak, multi-peak, and broadband absorbers [131-134].

#### **1.4. Composite based on magnetic-metamaterial electromagnetic wave absorbers**

MA typically exhibit single-peak or multi-peak absorption spectra with narrow bandwidths due to the LC-resonant nature of metallic structures. Meanwhile, magnetic materials often provide broadband loss, but it is difficult to achieve high absorption when the thickness is small. On this

basis, researchers have integrated magnetic materials into MA structures to improve and broaden the absorption spectrum by combining structural resonance in the MA and intrinsic losses in the magnetic material. Studies aiming to broaden the operating bandwidth and reduce the thickness of magnetic layers in the L (1-2 GHz), S (2-4 GHz), C (4-8 GHz), X (8-12 GHz), and Ku (12-18 GHz) bands have been conducted, including approaches using external lumped components and multilayer structures [136-138].

Research on applying an external magnetic field to CM-MA to tune the resonance frequency began in 2008, when Kang [31] proposed a metamaterial with negative permeability that could be controlled by a magnetic field. Subsequently, in 2009, Zhao and co-workers [143] combined YIG ferrite rods with metallic wires to realize broadband, dynamic, continuous, and reversible magnetic-field tunability. Huang and co-workers (2014) synthesized and experimentally demonstrated a magnetically tunable metamaterial absorber structure, employing a ferrite based magnesium (TT1-390) as the ferrite layer and a metallic metamaterial pattern on the surface, operating in the X band [32]. As  $H_0$  increased, the absorption peak near 10 GHz exhibited a clear frequency shift, while achieving an absorption approx 0.98 at various  $H_0$  values. In 2016, Li and colleagues proposed a metamaterial electromagnetic wave absorber operating in the 0.2 - 7.6 GHz range, using a YIG ferrite sheet as the substrate [27]. Experimentally varying  $H_0$  from 600 Oe to 1000 Oe shifted the absorption spectrum from 2.2 GHz to 3.2 GHz while maintaining high absorption [144].

### **1.5. Applications of composite based on magnetic-metamaterial**

CM-MA materials are an emerging class of materials that expand compositional diversity and enable broader electromagnetic absorption bandwidths. In electronics, CM-MA are used to mitigate electromagnetic interference (EMI) [149-151]. In addition, CM-MA have also been applied in defect-detection sensors [150].

### **1.4. Conclusion of Chapter 1**

This chapter presents the research status of CM-MA. Resonance

mechanisms and the impedance-matching principle have been discussed and analyzed to clarify the absorption mechanism of several CM-MA systems. The dissertation also summarizes CM-MA structures and research progress on tuning the absorption properties of CM-MA structures, and it introduces several representative applications of CM-MA in this chapter.

## **CHAPTER 2. RESEARCH METHODOLOGY**

### **2.1. Theoretical research method**

#### **2.1.1. Simulation methodology**

Specialized software packages such as CST Microwave Studio, HFSS, and COMSOL are commonly used to design and simulate MM. They allow for the simulation of materials in either 2D or 3D space. The electromagnetic properties of an MM can be determined by simulating a single unit cell structure, completely defining the parameters, material types, and appropriate boundary conditions.

#### **2.1.2. Impedance calculation method**

In MA structures, high absorption is essentially associated with two simultaneous conditions: impedance matching with free space/air to suppress reflection, and the presence of dielectric and/or magnetic losses to dissipate the incident energy. In this dissertation, the impedance of CM-MA is determined from the scattering parameters (S-parameters) obtained in simulations, serving as the basis for evaluating the degree of impedance matching and explaining the mechanism responsible for the formation of absorption peaks.

### **2.2. Fabrication and Measurement method for electromagnetic properties**

#### **2.2.1. High-energy mechanical milling**

The magnetic materials used in this dissertation were prepared by high-energy mechanical milling. High-energy milling belongs to the family of mechanical milling/mechanical alloying methods, in which the mechanical energy from the motion of the milling balls is transferred to powders through impacts, friction, and shear forces, producing severe plastic deformation and a high density of defects. Unlike many chemical synthesis

methods (which require solvent environments, pH control, complexing agents, etc.), mechanical milling is typically carried out via a solid-state route, which is advantageous for particle-size refinement, surface activation, and promoting the formation of equilibrium/non-equilibrium phases after subsequent heat treatment.

### **2.2.2 Measurement of permeability and permittivity**

The magnetic powder samples obtained were used to measure permittivity and permeability using a Keysight PNA-X N5242A network analyzer. The measured  $S_{11}$  and  $S_{21}$  parameters were then processed using the Nicolson-Ross-Weir algorithm [157] to calculate the relative permittivity ( $\epsilon_r$ ) and relative permeability ( $\mu_r$ ).

### **2.2.3. Vibrating sample magnetometry**

In this thesis, the magnetic parameters of the samples (the hysteresis loop  $M(H)$ , saturation magnetization, and coercivity) were determined using a vibrating sample magnetometer in order to evaluate the magnetic responsiveness of the materials.

### **2.2.4. Scanning electron microscopy**

The morphological structure of the magnetic materials used in this dissertation was investigated by scanning electron microscopy (SEM; Hitachi S4800, Japan) at the Institute of Materials Science. The field-emission SEM system is also equipped with an EMAX ENERGY energy-dispersive X-ray spectroscopy (EDX) unit, enabling elemental analysis over micrometer-scale regions.

### **2.2.5. X-ray diffraction**

X-ray diffraction was employed in this thesis to determine the single-phase nature of the materials.

## **2.3. Fabrication method for metamaterial and composite based on magnetic-metamaterial**

### **2.3.1 Photolithography for metamaterial fabrication**

For GHz-band MA structures, particularly three-layer metal - dielectric - metal configurations, the metallic resonator elements in the top layer (periodic metallic patterns) are typically subwavelength in size and

arranged periodically within a unit cell. Therefore, the core fabrication requirement is to produce accurate and uniform metallic patterns over the sample area, with minimal geometric deviation to limit undesired shifts in the resonant frequency. Photolithography is a standard patterning technique in microfabrication. The general photolithography process includes: exposure through a mask, development of the photoresist after exposure, metal etching to form the structure, and subsequent exposure and removal of the remaining photoresist to reveal the final pattern [122, 161].

### **2.3.2. Integration of magnetic materials onto metamaterials**

The as-prepared magnetic materials in powder form were mixed with binders and cast into thin sheets to serve as coating layers. The constituent layers were then assembled into a unified block using specialized binders such as epoxy or paraffin; after curing/solidification, they form flattened thin-film layers to ensure good adhesion.

### **2.4. Measurement method for electromagnetic properties of composite based on magnetic - metamaterial**

The Vector Network Analyzer (VNA) system at the Institute of Materials Science, Vietnam Academy of Science and Technology, is used to determine the reflectance of CM-MA. This system features two antennas serving as the source and receiver, whose positions are adjusted based on the required measurement. The output of the measurement is the complex S-parameters, which characterize the reflective and transmissive properties of the CM-MA.

### **2.4. Conclusion of Chapter 2**

The thesis employs high-energy mechanical milling combined with sintering to fabricate the magnetic materials. The experimentally obtained electromagnetic parameters (permeability and permittivity) of the magnetic materials, after measurement and calculation, are imported into CST Microwave Studio as an input database. The CM-MA structures are then designed and optimized. Based on the simulation results, the MA samples are fabricated by photolithography, and the magnetic materials are integrated onto the MA to form CM-MA structures using paraffin or epoxy as binders.

After fabrication, the electromagnetic properties of the samples are measured using a vector network analyzer (VNA) system.

## CHAPTER 3. RESEARCH ON BROADBAND ELECTROMAGNETIC WAVE ABSORBING COMPOSITE BASED ON FeCo-C MAGNETIC MATERIAL AND METAMATERIALS

### 3.1. Metamaterials using magnetic materials as resonant structures

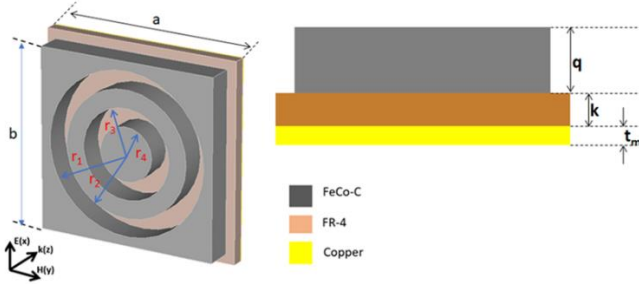


*Figure 3.1. CM-MA structure using magnetic materials as the resonant structure*

The structure comprises three layers: FeCo/graphite nanosheets (FeCo-C) whose shape looks like a flat sheet with two punched-in rings at the top, a middle layer of Flame Retardant 4 (FR-4), and a continuous copper plate at the bottom. In our simulation, we used a relative permittivity of FR-4 of 4.3, with a loss tangent of 0.025, and employed the copper layer with a conductivity of  $5.8 \times 10^7$  S/m [166].

The proposed structure exhibits a broadband absorption, with an absorption over 90% in a frequency range of 7.9 to 14.4 GHz, featuring two peaks with the near-unity absorption at 9.4 and 12.5 GHz, respectively [Fig. 3.6(a)]. The absorption spectrum of the CM-MA based FeCo-C was found to be significantly broader than that of the copper-backed FeCo-C, indicating an improvement in the absorption upon integrating the FeCo-C material into the metamaterial structure. To clarify the role of different layers in the metamaterial structure, the fractions of energy dissipated in the FeCo-C and FR-4 layer are presented in Fig. 3.6(b). It is shown that more than 98% of the energy loss occurred in the FeCo-C layer, while the loss in the FR-4 one was limited to be only 2%. The energy-dissipation results prove that the FeCo-C layer in CM-MA is the main factor contributing to the broadband absorption.

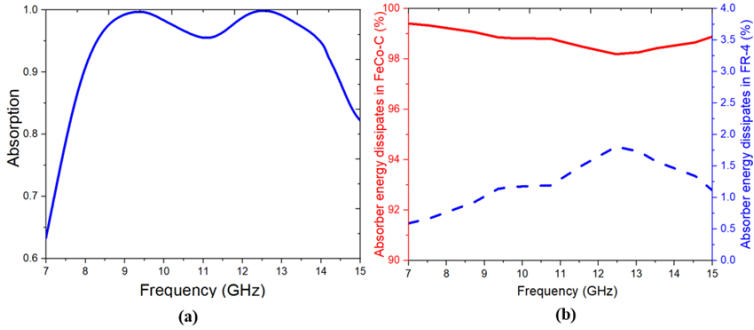


**Figure 3.6.** Absorption spectrum of the designed CM-MA structure and (b) the captured energy dissipated in the FeCo-C and FR-4 layer in the CM-MA structure.

It can be observed that the magnetic field is strongly excited at the corners of CM-MA structure. Specifically, the magnetic dipoles are seen along the direction of incident H-field with electric half vortices at the same positions. The observed phenomena suggest that the absorption mode at 9.4 GHz is due to a magnetic-dipole Mie-resonance, caused by the dielectric resonator [168, 169]. Similar, The CM-MA also exhibits the magnetic-dipole Mie-resonance at 12.5 GHz, as indicated by the strong magnetic dipoles along the H-direction and the electric half vortices in the  $(E, k)$  plane.

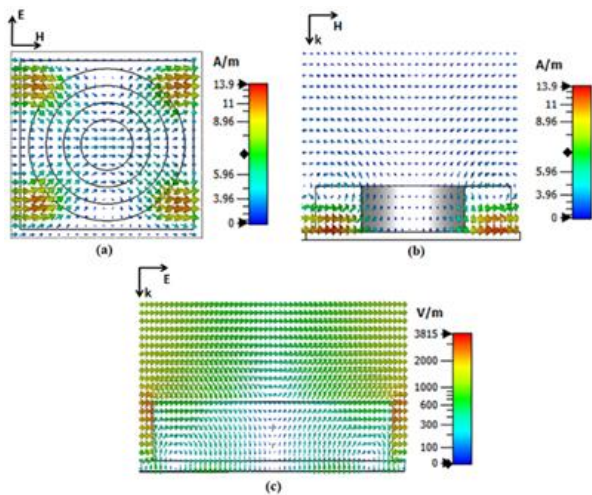


**Figure 3.7.** Electric- and magnetic-field distribution of the CM-MA structure. (a) Magnetic field in the  $(E, H)$  plane, (b) magnetic field in the  $(H, k)$  plane and (c) electric field in the  $(E, k)$  plane at a frequency of 9.4 GHz.

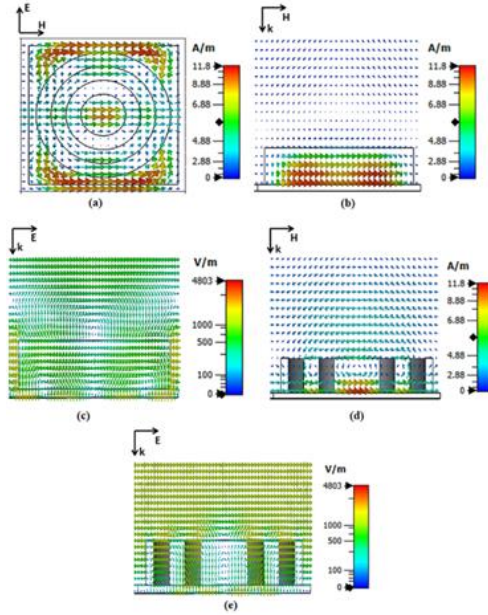


**Figure 3.8.** Electric- and magnetic-field distributions of the CM-MA structure at a frequency of 12.5 GHz. (a) Magnetic field in the  $(E, H)$  plane. (b) and (d) Magnetic field in the  $(H, k)$  plane. (c) and (e) Electric field in the  $(E, k)$  plane

### 3.2. Metamaterials using magnetic materials as a coating layer

The CM-MA structure has basic unit cell size of  $20 \times 20 \text{ mm}^2$  (Figure 3.17) and consists of four layer, with the top layer is a MM plate with a thickness of  $t_f$ , the middle layer of MA is copper composed of two punched-in rings with four edges are opened and the bottom layer is continuous copper plate.

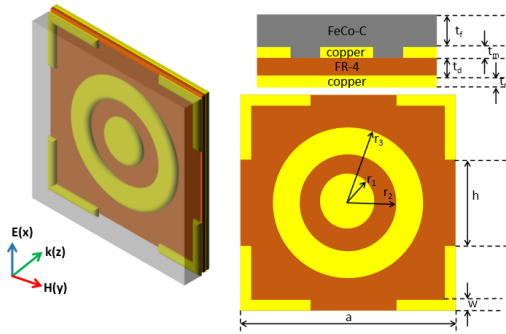


**Figure 3.17.** Schematic of CM-MA based FeCo-C.

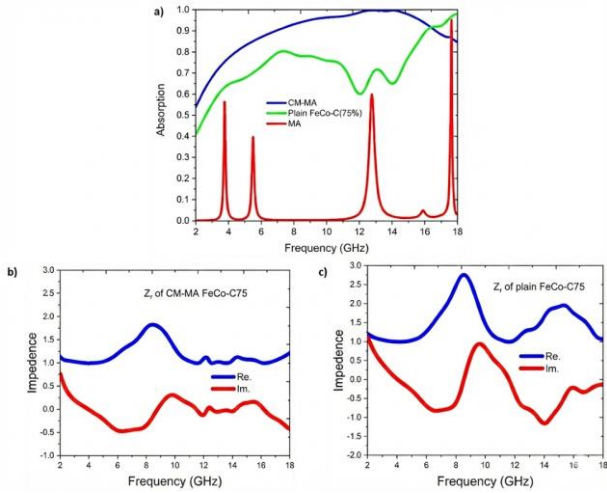


**Figure 3.22.** (a) Comparison of absorption spectra for magnetic materials, metamaterials and hybrid magnetic metamaterials FeCo-C (75%); (b-c) real and imaginary part of  $Z_r$ .

The results indicate that integrating FeCo-C (75%) into the CM-MA structure effectively enhances both the absorption bandwidth and absorption intensity compared with conventional materials. The proposed CM-MA structure exhibits a significantly broader absorption bandwidth of 9.9 GHz (from 6.9 to 16.8 GHz).

Observing the surface current distribution concentrated at the center circle, partly at the outer circle and at the L-shaped lines. It is evident that the surface current on the metal pattern aligns inversely parallel to the metal substrate, forming a magnetic dipole resonance..

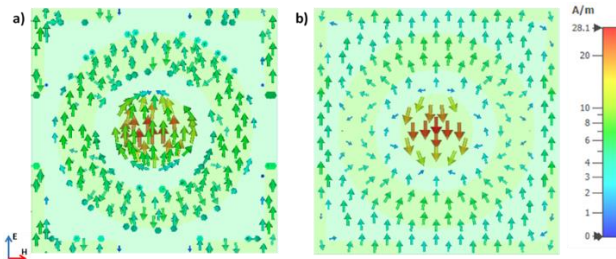


**Figure 3.24.** The surface current on the (a) the top metal patten and (b) bottom metal backplane at 13.5 GHz of HMA based FeCo-C (75%).

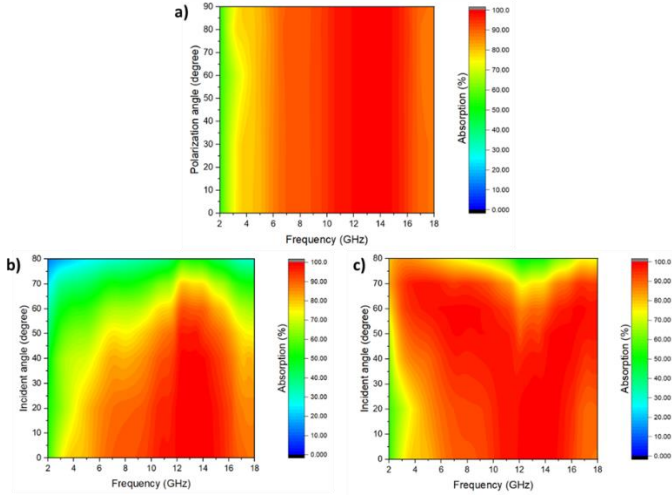


**Figure 3.24.** Dependence of the absorption spectrum of CM-MA on the (a) polarization angle at the normal incidence, and incident angle in the (b) TE and (c) TM polarization.

A study on the structural stability under variations in the incidence angle and polarization angle shows that the structure is almost unaffected by the polarization angle [Fig. 3.24 (a)]. The CM-MA structure still exhibits good absorption performance under both TE and TM polarizations, even at large incidence angles. Specifically, in the TM polarization, the absorption decreases as the incidence angle increases from  $0^\circ$  to  $70^\circ$ , but it remains higher than 90% over the 6.9 - 12 GHz band [Figure 3.24(c)], with an FBW of 59.46%. In the TE mode, the absorption is maintained above 90% in the 11.5-16.3 GHz range for incidence angles up to  $40^\circ$  [Figure 3.24(b)], while the FBW of the CM-MA decreases to 34.53%.

Five CM-MA samples were fabricated with different carbon-FeCo ratios: 10%, 50%, 75%, 90%, and pure graphene. The experimental results are presented in Figure 3.26. It can be observed that as the carbon content increases from 10% to 75%, the absorption spectrum of the structure is enhanced in both absorption intensity and bandwidth. However, when the carbon content increases to 90% and 100% carbon (without using magnetic material), the absorption intensity of the structure tends to decrease. Overall,

the simulation and experimental results are in good agreement.

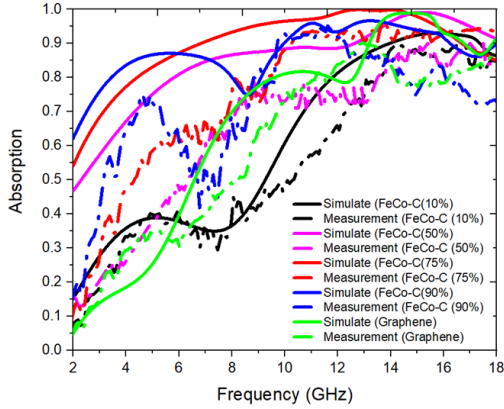


**Figure 3.27.** Comparison of absorption (for simulated and measurement) spectra for HMA with different carbon to FeCo ratios: 10%, 50%, 75%, 90%, and pure graphene, respectively.

The dissertation also performed simulations of integrating FeCo–C (10%) into a CM-MA structure featuring an H-shaped resonant pattern, with the aim of enhancing and broadening the absorption frequency range of FeCo-C (10%).

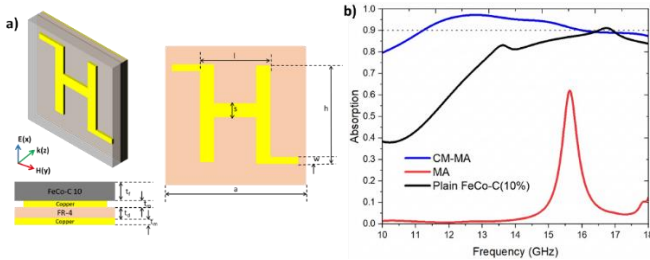


**Figure 3.31.** (a) Schematic of CM-MA based FeCo-C (10%) unit cell, (b) Comparison of absorption spectra for plain FeCo-C(10%), MA and CM-MA.

The results indicate that the integrating FeCo-C material into the MA effectively extends both the absorption frequency range and the absorption compared to conventional FeCo-C(10%) with an equivalent thickness. The proposed CM-MA based FeCo-C exhibits a significantly broader absorption bandwidth EAB of 4.8 GHz (ranging from 11.2 to 16 GHz) with a peak absorption of nearly 100% at 12.8 GHz, and a substantially

expanded FBW of 35.29%.

Illustrate the surface current at 12.8 GHz shown that the surface current on the metal pattern aligns inversely parallel to the metal substrate, forming a magnetic dipole resonance.

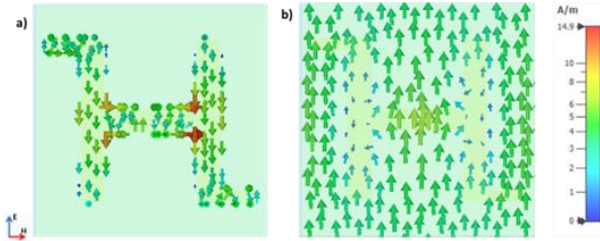


**Figure 3.34.** The power-loss density in the cross section of the (a-b) in the  $(E, H)$  plane on the metal pattern, (c) in the  $(k, E)$  plane at 12.8 GHz of CM-MA based FeCo-C(10%).

### 3.3. Conclusion of Chapter 3

- The CM-MA structure using FeCo-C as the resonant element was designed and simulated, demonstrating broadband absorption with absorption above 90% in the 7.9 - 14.4 GHz range. The absorption is well maintained under both TE and TM polarizations when the incidence angle varies from  $0^\circ$  to  $55^\circ$ .

- CM-MA structure employing FeCo-C as an absorbing coating layer was designed, simulated, and fabricated using five different carbon ratios: 10%, 50%, 75%, 90%, and pure graphene, coated on an MA structure perforated with two circular holes. For the optimal carbon ratio of 75%, the structure exhibits absorption above 90% with a wide absorption bandwidth of 9.9 GHz (simulation) and 7.7 GHz (measurement). The structure is almost insensitive to the polarization angle. It maintains good absorption performance as the incidence angle increases under both TE (up to  $40^\circ$ ) and TM polarizations, with better angular stability in the TM mode (up to  $70^\circ$ ).

- CM-MA structure using FeCo-C (10%) as a coating layer on an H-shaped MA was designed and simulated for broadband electromagnetic wave absorption. The structure achieves absorption above 90% in the 11.2-16 GHz band. The CM-MA with FeCo-C (10%) also maintains good absorption characteristics for both TE and TM incident-wave polarizations.

## CHAPTER 4. STUDY ON MODULATING THE AMPLITUDE AND TUNNING FREQUENCY OF ELECTROMAGNETIC WAVE ABSORPTION OF COMPOSITE BASED ON MAGNETIC MATERIALS BASED ON $MFe_2O_4$ AND METAMATERIALS

### 4.1. Modulate the absorption intensity of composite materials

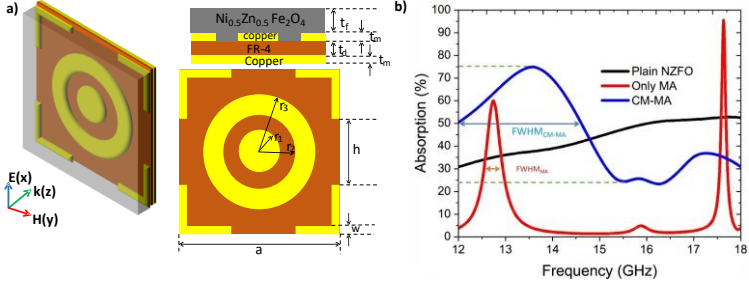


**Figure 4.2.** (a) Schematic of CM-MA based NZFO unit cell, (b) Comparison of absorption spectra for NZFO materials, MA and CM-MA based NZFO.

The results indicate that the integration of the NZFO material into the metamaterial structure effectively broadens the absorption frequency range compared to the conventional material. For the conventional NZFO material of the same thickness as the CM-MA, the electromagnetic wave absorption ranges from approximately 30% to 51% within the investigated frequency range. For the MA without the NZFO material, there is only one absorption peak at 17.8 GHz with an absorption of about 96% and another peak at 12.9 GHz with an absorption lower than 60% with FWHM approximately 0.5 GHz. In contrast, the proposed CM-MA exhibits broader absorption bandwidth, with an absorption peak approximately 75% and the FWHM is enhanced to be approximately 4.6 GHz.

To clarify the absorption mechanism, the dissertation investigated the surface current distribution at the absorption peak of 13.59 GHz. The results show that, the surface current is concentrated at the outer circle, partly at the central circle and the L-shaped edges at the corners of the structure. Here, the surface current at the metal layer is parallel and opposite to the current at the bottom layer, forming a magnetic dipole resonance that results in strong

absorption of the incident wave and the formation of the absorption peak.

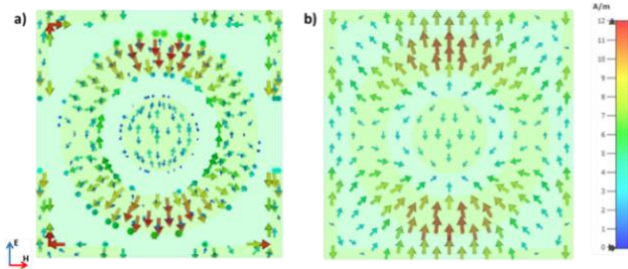


**Figure 4.6.** The surface current on the (a) the top metal patten, (b) bottom metal backplane,

The absorption amplitude of the CM-MA structure is enhanced from 75% to 97% as the external magnetic field applied to the structure is increased from 0 to 2000 Oe.

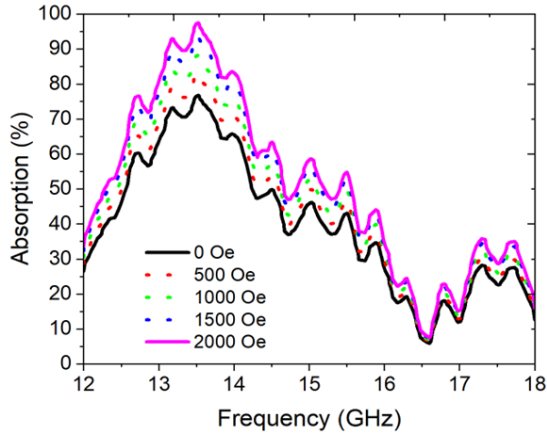


**Figure 4.11.** Absorption spectrum of CM-MA structure when the intensity is varied from 0 to 2000 Oe

#### 4.2. Influence of the dielectric on the interaction

The CM-MA has a unit-cell size of  $20 \times 20 \text{ mm}^2$  (Figure 4.16) and consists of five layers, with the top layer being an  $\text{MgFe}_2\text{O}_4$  slab studied by HuangYoung Jun and co-workers (2014) in publication [32].

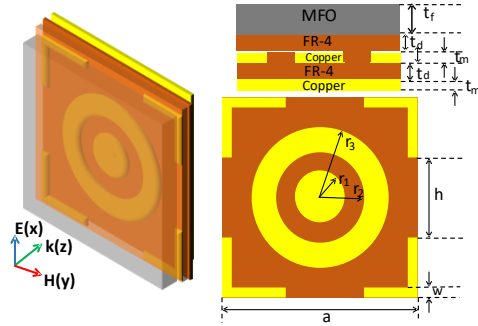


**Figure 4.16.** Schematic of CM-MA based MFO unit cell.

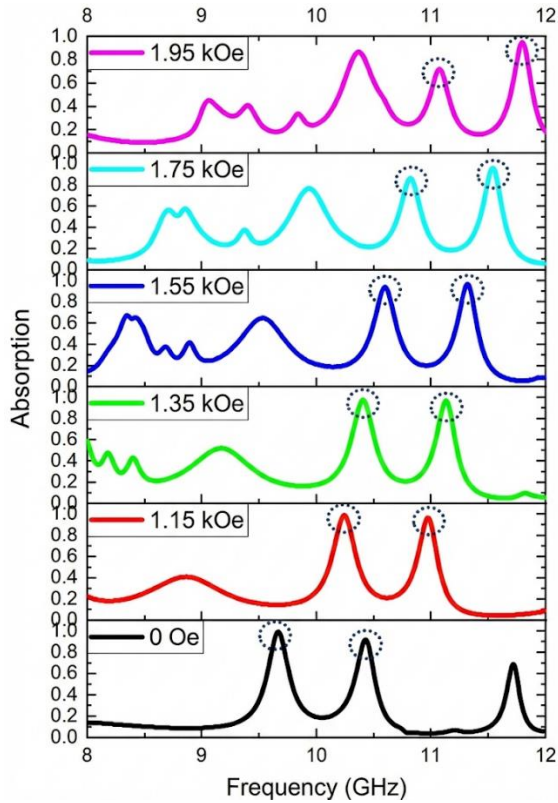


**Figure 4.18.** The absorption spectrum of the CM-MA structure using MFO under external magnetic fields of 0 Oe, 1.15 kOe, 1.35 kOe, 1.55 kOe, 1.75 kOe, and 1.95 kOe, respectively.

The results show that the CM-MA structure exhibits two absorption peaks whose frequencies can be tuned over relatively wide ranges: 1.42 GHz (from 9.66 GHz to 11.08 GHz) for the first peak and 1.37 GHz (from 10.43 GHz to 11.80 GHz) for the second peak, as the applied external magnetic field is varied from 0 to 1.95 kOe.

### **4.3. Conclusion of Chapter 4**

- NZFO was fabricated and integrated into the MA structure, leading to enhanced absorption intensity and a broadened absorption spectrum compared with the MA alone and the standalone NZFO material. The absorption amplitude of the CM-MA structure increases from 75% to 97% as the external magnetic field is varied from 0 to 2000 Oe. The absorption-amplitude tuning mechanism is attributed to the increase in the real part of NZFO permeability with the applied magnetic field, which modifies the overall impedance of the CM-MA around the absorption frequency of 13.59 GHz.

- The frequency-tuning capability of a CM-MA structure using MFO was designed and simulated. The MFO-based CM-MA exhibits a multi-peak absorption spectrum with absorption above 90% and enables tuning of the absorption frequencies within the X-band. As the applied external magnetic field increases from 0 to 1.95 kOe, the tunable frequency range is relatively wide, reaching 1.42 GHz (from 9.66 GHz to 11.08 GHz) for the first peak and 1.37 GHz (from 10.43 GHz to 11.80 GHz) for the second peak.

### **Overall Conclusion**

The dissertation focuses on investigating the broadband electromagnetic-wave absorption characteristics of CM-MA structures, while also studying approaches to modulate the absorption amplitude and tuning frequency in order to improve performance and flexibility.

- CM-MA using FeCo-C as the resonant structure was designed and simulated, demonstrating broadband absorption with absorption above 90% in the 7.9 - 14.4 GHz range. The absorption remains above 90% over a wide

incidence-angle range from  $0^\circ$  to  $55^\circ$  under both TE and TM polarizations.

- A broadband CM-MA structure employing FeCo-C with five different carbon ratios (10%, 50%, 75%, 90%, and pure graphene) was successfully designed, simulated, and fabricated. For the optimal carbon ratio of 75%, the structure exhibits absorption above 90% with a wide absorption bandwidth spanning the C-Ku band (6.9 - 16.8 GHz). The structure maintains good absorption performance as the incidence angle varies; under TM polarization it shows better angular stability than under TE polarization.

- CM-MA structure using  $\text{Ni}_{0.5}\text{Zn}_{0.5}\text{Fe}_2\text{O}_4$  was fabricated, and the absorption amplitude at 13.59 GHz was tuned from 75% to 97% by gradually increasing the external magnetic field applied to the structure up to 2000 Oe.

- CM-MA structure integrated with  $\text{MgFe}_2\text{O}_4$  was designed to achieve multi-peak absorption in the X-band with magnetic-field-controlled frequency tunability. The tuning range is relatively wide, reaching 1.42 GHz (from 9.66 GHz to 11.08 GHz) for the first peak and 1.37 GHz (from 10.43 GHz to 11.80 GHz) for the second peak as the applied magnetic field is increased up to 1950 Oe.

### **FUTURE RESEARCH DIRECTIONS**

1. Use machine learning techniques and AI to optimize CM-MA structures.
2. Apply emerging fabrication techniques and integrate advanced materials in the development of CM-MA. To develop novel magnetic material systems exhibiting high absorption, broad absorption bandwidth, and tunable absorption frequencies with a wide tuning range.
3. Research and apply CM-MA structures for EMI shielding and sensing applications such as defect inspection and detection.

## LIST OF PUBLICATIONS RELATED TO THE THESIS

1. **Tang Xuan Duong**, Do Khanh Tung, Pham Thanh Son, Nguyen Hai Anh, Bui Son Tung, Nguyen Phon Hai, Vu Thi Hong Hanh, Tran Quang Dat, Bui Xuan Khuyen, and Vu Dinh Lam. "Broadband metamaterial absorber in the C-Ku bands by exploiting FeCo-C." *Journal of Applied Physics* 137, no. 6 (2025).
2. **Tang Xuan Duong**, Do Khanh Tung, Bui Xuan Khuyen, Nguyen Thi Ngoc Anh, Bui Son Tung, Vu Dinh Lam, Liangyao Chen, Haiyu Zheng, and YoungPak Lee. "Enhanced electromagnetic wave absorption properties of FeCo-C alloy by exploiting metamaterial structure." *Crystals* 13, no. 7 (2023): 1006.
3. Tang Xuan Duong, Do Khanh Tung, Nguyen Hai Anh, Bui Son Tung, Dao Son Lam, Bui Xuan Khuyen and Vu Dinh Lam, "Enhanced and modulated Ku-band absorption of a hybrid  $\text{Ni}_{0.5}\text{Zn}_{0.5}\text{Fe}_2\text{O}_4$  metamaterial structure", TNU Journal of Science and Technology, 2026.
4. Granted patent: Do Khanh Tung, Bui Xuan Khuyen, Bui Son Tung, Nguyen Thanh Huong, Vu Dinh Lam, **Tang Xuan Duong**, "Broadband electromagnetic wave absorbing modified material based on FeCo-C", Patent No.: 56247, Application number: 1-2023-08775, Decision No. 16470/QD-SSTT-IP dated February 03, 2026 of the Intellectual Property Office..
5. **Tang Xuan Duong**, Do Khanh Tung, Bui Son Tung, Vu Dinh Lam, Bui Xuan Khuyen, "Metamaterial utilizing FeCo/Graphite alloy for absorbing electromagnetic waves in the GHz frequency range", Proceedings of IWNA, 08-11 (2023).
6. **Tang Xuan Duong**, Do Khanh Tung, Pham Thanh Son, Nguyen Hai Anh, Nguyen Van Ngoc, Nguyen Thanh Tung, Bui Son Tung, Vu Thi Hong Hanh, Vu Dinh Lam, Young Park Lee, and Bui Xuan Khuyen, "Enhanced and expanded the absorption in the GHz frequency range by integrating magnetic materials into the metamaterial structure", Proceedings of IWAMSN 2024, 22-25 September (2024).